

# Hydrogen bonding and tautomerism of benzylideneanilines in the solid state

Dorota Maciejewska,<sup>1\*</sup> Dorota Pawlak<sup>2</sup> and Vera Koleva<sup>3</sup>

<sup>1</sup>Department of Physical Chemistry, Faculty of Pharmacy, Medical University of Warsaw, Banacha 1, 02-097 Warsaw, Poland

<sup>2</sup>Faculty of Chemistry, University of Warsaw, Pasteura 1, 02-093 Warsaw, Poland

<sup>3</sup>Faculty of Chemistry, University of Sofia, Sofia 1126, Bulgaria

Received 31 January 1999; revised 25 March 1999; accepted 7 September 1999

**ABSTRACT:** The <sup>13</sup>C cross-polarization magic angle spinning NMR spectra of *N*-(2'-hydroxybenzylidene)-2-hydroxyaniline (**1**), *N*-(2'-hydroxybenzylidene)-4-nitroaniline (**2**) and *N*-(4'-dimethylaminobenzylidene)-2-hydroxyaniline (**3**) indicate a keto–hydroxy tautomerism of **1** but not of **2**. This was confirmed by a single-crystal x-ray diffraction study of **1**, which revealed that the two distinct molecules in the unit cell are linked by intermolecular hydrogen bonding. The presence of this bonding may explain the occurrence of the keto–hydroxy tautomerism. Copyright © 1999 John Wiley & Sons, Ltd.

**KEYWORDS:** benzylideneanilines; hydrogen bonding; keto–hydroxy tautomerism

## INTRODUCTION

Molecules with the general formula >C=N–Ph are known as Schiff bases.<sup>1</sup> They have wide application in organic synthesis and exhibit thermochromism and photochromism.<sup>2,3</sup> They constitute an interesting model for theoretical studies of intra- and/or intermolecular hydrogen bonding.

Different proton transfer phenomena can occur even in the solid state and diffraction methods are able to distinguish between the various tautomers. Studies<sup>4</sup> of phenol–imine and keto–amine tautomers show the C–O bond to be much longer in the former (1.341 Å) than in the latter (1.234 Å). The aniline ring is not coplanar with the second ring in the keto–amine tautomer, and the nitrogen atom completing the hydrogen bond has largely sp<sup>3</sup> character.

<sup>13</sup>C and <sup>15</sup>N cross-polarization magic angle spinning (CP/MAS) NMR spectroscopy is a complementary technique for the detection of the possible dynamic processes. The methods for the determination of tautomeric equilibrium<sup>5</sup> are based on an arbitrary choice of the model compounds for both tautomers. <sup>1</sup>H, <sup>13</sup>C and <sup>15</sup>N chemical shifts or various coupling constants have been proposed for the estimation of the tautomer content. The results of such an approach have been published for the HO-bearing benzylideneanilines and azo derivatives in solution.<sup>6–10</sup> The proposed structures showed an H···N intramolecular hydrogen bond, with the proton

located near the oxygen atom in phenyl derivatives but near the nitrogen atom in naphthyl or heterocyclic compounds.

In this work, three benzylidene anilines with an *ortho* OH substituent at one of the aromatic rings or both (see Fig. 1) were examined using <sup>13</sup>C CP/MAS NMR spectroscopy, IR measurements, x-ray diffraction (XRD) and semi-empirical MO calculations. The aim was to acquire structural information on hydrogen bonding and possible keto–hydroxy tautomerism in the benzylideneanilines. The most interesting features of the hydrogen bonding in **1** and **2** are the variations of the H-atom position in the intramolecular hydrogen bridge and the interaction of the second OH group with the adjacent molecules in **1** (see Fig. 2). The electron-withdrawing substituent in **2** should increase the stability of a keto tautomer. The derivative **3** could be a model of the chemical shifts for a hydroxy tautomer, forming only an intermolecular hydrogen bond. The electron-donating substituent in the *para* position was expected to stabilize such a form. The structure of **1** in the solid state has already been established by XRD.<sup>11</sup> The structure was refined in the C2/c space group, with the result *R*<sub>1</sub> = 0.09. There were two different molecules in the independent part of the unit cell, and in one of those molecules both oxygen atoms were disordered between two positions. The structure extracted from our x-ray study is different to those determined previously.

## EXPERIMENTAL

The three compounds studied were synthesised as

\*Correspondence to: D. Maciejewska, Department of Physical Chemistry, Faculty of Pharmacy, Medical University of Warsaw, Banacha 1, 02-097 Warsaw, Poland.  
E-mail: domac@farm.amwaw.edu.pl

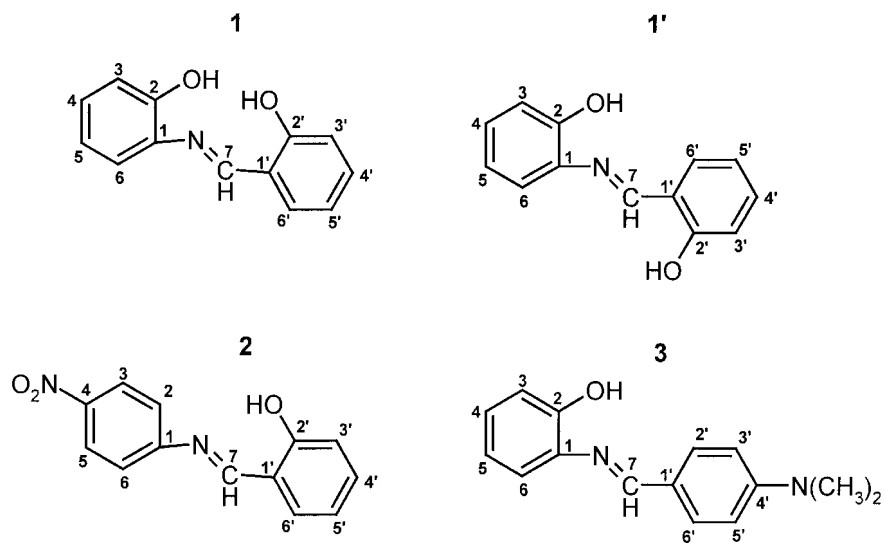


**Figure 1.** Benzylideneanilines **1–3**

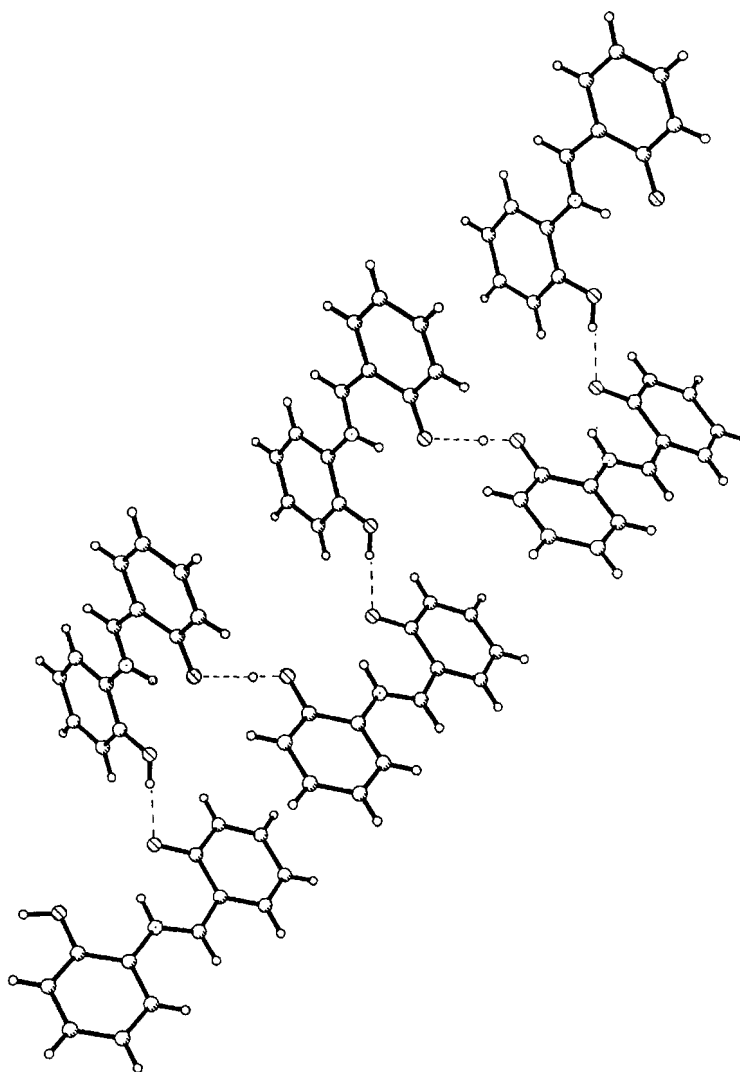


**Figure 2.** Hydrogen-bonded chains of **1**

**Table 1.** Crystal data and structure refinement for **1**

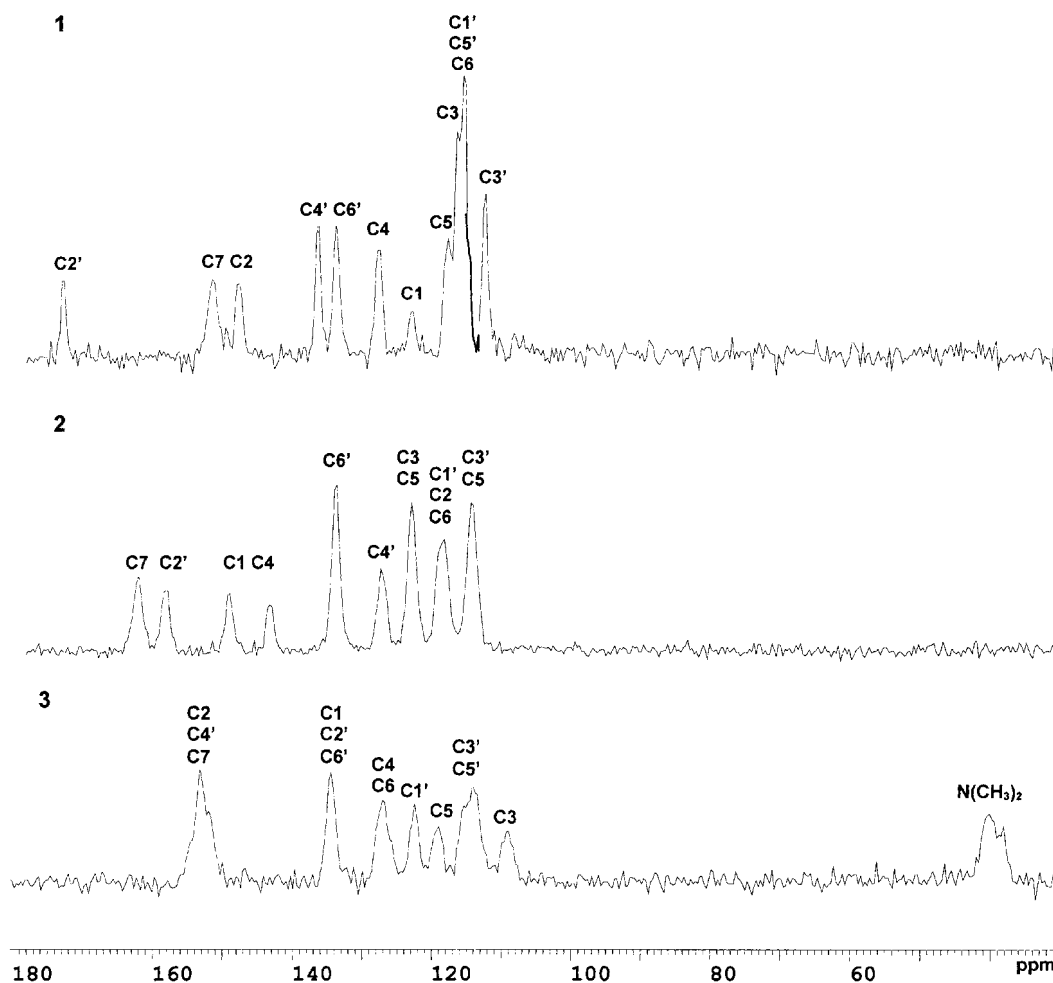
$C_{13}H_{11}NO_2$	$F(000)$ 448
$M_r = 213.23$	Theta range for data collection: 3.87–85.24°
Triclinic	Index ranges: $-11 \leq h \leq 10$ , $-12 \leq k \leq 12$ , $0 \leq l \leq 14$
$P-1$	Reflections collected: 4395
$a = 8.985(2) \text{ \AA}$ , $\alpha = 69.43(3)^\circ$	Independent reflections: 4201 [ $R(\text{int}) = 0.0577$ ]
$b = 10.052(2) \text{ \AA}$ , $\beta = 89.91(3)^\circ$	Refinement method: full-matrix least-squares on $F^2$
$c = 12.255(2) \text{ \AA}$ , $\gamma = 77.01(3)^\circ$	Data/restraints/parameters: 4201/0/330
$1006.1(3) \text{ \AA}^3$	Goodness-of-fit on $F^2$ : 1.051
$Z = 4$	Final $R$ indices [ $I > 2\sigma(I)$ ]: $R_1 = 0.0540$ , $wR_2 = 0.1605$
$D_x = 1.408 \text{ mg m}^{-3}$	$R$ indices (all data): $R_1 = 0.0656$ , $wR_2 = 0.1701$
$\mu = 0.778 \text{ mm}^{-1}$	Extinction coefficient: 0.0118(15)
$\lambda = 1.54178 \text{ \AA}$	Largest difference peak and hole: 0.348 and $-0.278 \text{ e \AA}^{-3}$
$T = 293(2) \text{ K}$	

described earlier.<sup>12</sup>  $^{13}\text{C}$  NMR spectra were recorded on a Varian Unity 200 MHz spectrometer in DMSO.  $^{13}\text{C}$  CP/MAS NMR spectra were recorded on a Bruker MSL 300 instrument at 75.5 MHz. Powdered samples were packed into a  $\text{ZrO}_2$  rotor and spun at about 10 KHz. A contact time of 5 ms, a repetition time of 6 s and a spectral width of 20 KHz were used for the accumulation of 800–1200 scans. The dipolar dephased spectra were

recorded with a 50  $\mu\text{s}$  delay before acquisition. The chemical shifts were calibrated indirectly through the glycine CO signal observed at 176.3 ppm relative to TMS.

Semi-empirical calculations were performed using the PM3 program as implemented in MOPAC 6.0.

X-ray diffraction measurements were made on a KUMA diffractometer with graphite-monochromated

**Figure 3.**  $^{13}\text{C}$  CP/MAS NMR spectra of solids **1–3**

**Table 2.**  $^{13}\text{C}$  NMR chemical shifts of **1–3** in solids and in DMSO (**1, 2**) and  $\text{CDCl}_3$  (**3**) solution (in parentheses)

No.	C(1)	C(2)	C(3)	C(4)	C(5)	C(6)	C(7)	C(1')	C(2')	C(3')	C(4')	C(5')	C(6')
<b>1</b>	124.56 (134.96)	150.11 (150.97)	118.00 (116.60)	129.39 (127.88)	119.23 (119.52)	116.86 (119.56)	153.87 (161.61)	116.86 (119.46)	175.74 (160.62)	113.84 (116.47)	138.44 (132.69)	116.86 (118.62)	135.78 (132.17)
<b>2</b>	150.99 (154.50)	119.75 (122.33)	124.32 (124.90)	145.02 (145.33)	124.32 (124.90)	119.75 (122.33)	164.25 (165.43)	119.20 (119.31)	160.27 (160.16)	115.54 (116.66)	128.71 (132.31)	115.54 (119.31)	135.52 (134.16)
<b>3</b>	134.44 (136.64)	153.20 (152.67)	108.49 (114.37)	127.03 (119.90)	118.88 (115.62)	127.05 (127.32)	153.20 (157.12)	122.42 (124.02)	134.44 (130.52)	114.02 (111.55)	153.20 (151.92)	114.02 (111.55)	134.44 (130.52)

$\text{CuK}_\alpha$  radiation at room temperature, using  $\omega$ – $2\theta$  scan techniques. The intensity of the control reflections varied by less than 5% and a linear correction factor was applied to account for this effect. The data were corrected for Lorentz and polarization effects and for absorption.<sup>13</sup> The structure was solved by direct methods<sup>14</sup> and refined using SHELXL.<sup>15</sup> The non-hydrogen atoms were refined anisotropically, whereas the H atoms were placed in calculated positions and their thermal parameters were refined isotropically. Positional and thermal parameters were refined only for those hydrogen atoms involved in hydrogen bonding. Atomic scattering factors were taken from the International Tables.<sup>16</sup> Crystal data and structure refinement for **1** are given in Table 1.

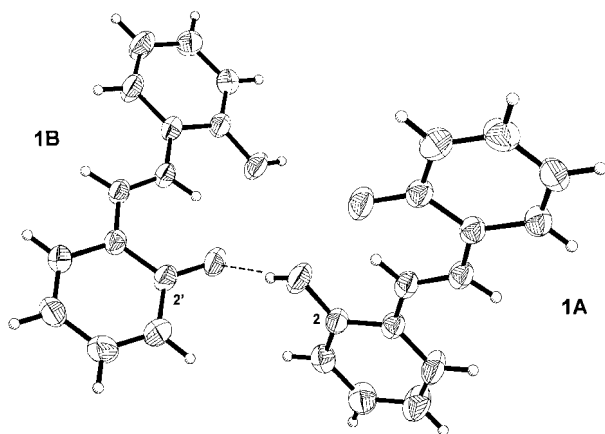
All positional, geometric and thermal parameters and the observed and calculated factors are deposited at the Cambridge Crystallographic Data Centre (CCDC Identification Number 133285).

The solid-state IR spectra were recorded in dry potassium chloride using a Nicolet 10MX FTIR spectrometer at  $2\text{ cm}^{-1}$  resolution with 60 scans.

## RESULTS AND DISCUSSION

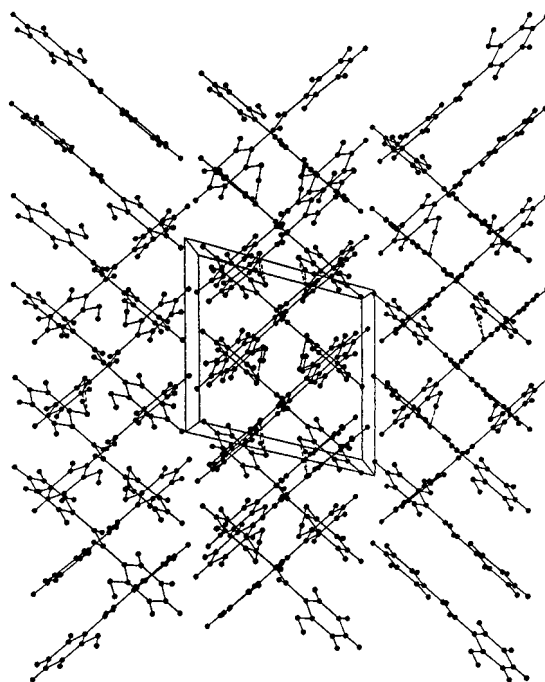
### NMR spectra

The  $^{13}\text{C}$  CP/MAS NMR spectra of **1–3** are shown in Fig. 3. The detailed assignments were made from the dipolar-

**Figure 4.** The displacement ellipsoids of **1A** and **1B**

dephased spectra, which reveal the resonances from quaternary and methyl carbon atoms, and by comparison with the spectra in solution. The spectra of structurally related compounds<sup>6–10</sup> and 2D NMR spectra of  $^1\text{H}$ – $^{13}\text{C}$  in solution were also helpful. The assignments are given in Table 2.

The examination of the spectrum of **1** indicates that there are significant differences between carbons C2 and C2'. In particular, the signals in solution are located at 150.97 ppm for C2 and at 160.62 ppm for C2', whereas the resonances of the solid sample were determined to be at 150.1 and 175.7 ppm, respectively. This is indicative of significant differences in electronic structure, *i.e.* the C2'–OH group is better represented as C2'=O $\cdots$ H because of the proton transfer. This is confirmed by the single-crystal XRD study of **1** in which the proton of the C(2')–OH group is located closer to the nitrogen atom than to oxygen. Such a structure is stabilized by the intermolecular hydrogen bonding system illustrated in Fig. 2. For the derivative **2** this proton transfer does not

**Figure 5.** A perspective drawing of the packing arrangement of **1**

**Table 3.** Bond lengths (Å) and selected valence angles (°) for **1**

Bond lengths of <b>1A</b>		Bond lengths of <b>1B</b>	
C(1)—C(2)	1.388(2)	C(1)—C(2)	1.384(2)
C(1')—C(2')	1.422(2)	C(1')—C(2')	1.420(2)
C(2')—C(3')	1.403(2)	C(2')—C(3')	1.411(3)
C(2)—C(3)	1.377(2)	C(2)—C(3)	1.379(2)
N(1)—C(7)	1.288(2)	N(1)—C(7)	1.284(2)
C(1)—C(6)	1.378(2)	C(1)—C(6)	1.373(2)
C(1')—C(6')	1.401(2)	C(1')—C(6')	1.400(2)
C(3)—C(4)	1.369(2)	C(3)—C(4)	1.361(3)
C(3')—C(4')	1.359(3)	C(3')—C(4')	1.347(3)
Valence angles of <b>1A</b>		Valence angles of <b>1B</b>	
C(2)—C(1)—N(1)	117.05(13)	C(2)—C(1)—N(1)	116.78(14)
C(2')—C(1')—C(7)	120.86(15)	C(2')—C(1')—C(7)	120.60(14)
O(2)—C(2)—C(1)	117.26(15)	O(2)—C(2)—C(1)	117.81(15)
O(2')—C(2')—C(1')	121.29(15)	O(2')—C(2')—C(1')	121.71(15)
N(1)—C(7)—C(1')	123.21(14)	N(1)—C(7)—C(1')	122.93(14)
C(7)—N(1)—C(1)	127.24(13)	C(7)—N(1)—C(1)	126.97(13)
C(3')—C(2')—C(1')	116.76(16)	C(3')—C(2')—C(1')	115.99(15)
C(3)—C(2)—C(1)	119.52(15)	C(3)—C(2)—C(1)	119.05(15)

take place and the chemical shifts of C2' in the solution and in the solid are almost equal.

The next striking difference between the solution and the solid is the change in the chemical shifts for the C7 atom. The resonance of the C7 atom in **1** moves to higher field by 7.4 ppm, closer to the limit for the ketoamine tautomer. The spectra of **2** and **3** contain significantly fewer peaks than the number of chemically distinct carbon sites in the molecules. It is possible that a 'flipping' motion of aromatic rings occurs which results in equivalence of the resonances of the *ortho* and *meta* pairs. Residual splitting could be observed for the resonance of the dimethylamino group in the spectrum of **3**, due to the dipolar coupling of the carbon atom linked to the quadrupolar  $^{14}\text{N}$  nitrogen atom. This splitting was not observed for the remaining C—N atoms.

### X-ray diffraction

Compound **1** crystallizes in the space group *P*-1 with two molecules (**1A**, **1B**) in the independent part of the unit cell as presented in Fig. 4. Figure 2 shows that chains of molecules are stabilized by the intermolecular hydrogen bonds, and the packing scheme is illustrated in Fig. 5. The

bond lengths and valence angles are given in Table 3. The apparent rigidity of the benzylidene moiety and non-planarity of the aniline moiety [the torsion angle is  $9.7(3)^\circ$ ] are increased by the strong intramolecular hydrogen bonding between the parent molecules, and also by the hydrogen bonding with adjacent molecules in a perpendicular chain. The hydrogen atom of the C2'—OH group (see Fig. 1) is localized near the nitrogen atom and the system is stabilized by the intramolecular hydrogen bond N—H $\cdots$ O. Structural parameters characterizing the hydrogen bonds are listed in Table 4.

The C2'—O bond is shortened and differs significantly from the typically single the C2—O bond, indicating the keto—amine conformation of the molecule **1**. The O $\cdots$ N distance is longer (by 0.064 Å) in the aniline moiety than the benzylidene moiety, and the hydrogen atom is localized near the oxygen atom. Consequently, this hydrogen atom is engaged in intermolecular H-bonding with the oxygen atom of the O—C2' group in an adjacent molecule. The quasi-aromatic ring N1 $\cdots$ H $\cdots$ O—C2'—C1'—C7, formed as a result of the intramolecular hydrogen bond, deviates only slightly from planarity. The hydrogen bonds are fairly strong and the energies calculated on the basis of the empirical equation  $E = 468.9\exp[4.338(0.957 - R_{\text{OH}})]^{17}$  are given in Table

**Table 4.** Crystal data for the hydrogen bonds in the molecules of **1A** and **1B**

Molecule	Distance (Å)				Calculated energies of hydrogen bond (kJ mol $^{-1}$ )		Valence angles (°) intra molecular N—H $\cdots$ O
					intra molecular NH $\cdots$ OC(2')	inter molecular C(2)OH $\cdots$ O	
	NH $\cdots$ O	C(2')—O	C(2)—O	C(2)OH $\cdots$ O			
<b>1A</b>	1.760(4)	1.286(2)	1.343(2)	1.715(4)	14.40(0.06)	17.50(0.07)	144.5(5)
<b>1B</b>	1.799(4)	1.278(2)	1.339(2)	1.607(4)	12.16(0.05)	27.96(0.12)	140.5(5)

4. Both phenyl rings vary in aromaticity. We observe 'equalization' of the bond lengths in the aniline ring and all bond lengths are slightly shorter than the ideal bond length of 1.388 Å. The HOMA parameter<sup>18</sup> describing aromaticity, which has a value of 1.000 for benzene, is equal to 0.951 for **1A** and 0.926 for **1B**. In the benzylidene moiety bond alternation is evident: the HOMA index for **1A** is 0.844 and for **1B** it is 0.797. Such a difference in aromaticity of two benzene rings in one molecule is caused by different substituents (HO—C in one case and O=C in the other).

## IR spectroscopy

The bent hydrogen bridge formed in the crystalline state is reflected in the IR spectrum of **1**, where the broad stretching vibration band is located at 2575 cm<sup>-1</sup> and the overtone of the bending vibration band appears at 1900 cm<sup>-1</sup>. The observed broad band of the stretching vibration  $\nu_{\text{OH}}$  with a maximum at 3450 cm<sup>-1</sup> in the spectra of **1** and **2** and at 3335 cm<sup>-1</sup> in that of **3** is a characteristic feature of hydrogen-bonded compounds. The larger shift towards lower wavenumbers and the increase in the intensity occurring in the spectrum of **3** are in line with the formation of stronger hydrogen bonding.

## Semi-empirical MO calculations

The calculations on **1** indicate that the key differences between the proposed structures are the orientation of the hydroxyl groups with respect to the C7—N linking bond, and the position of the hydroxyl protons. It appears that conformers with their OH groups on opposite sides of the C7—N bond, the structures **1** and **1'** in Fig. 1, are slightly less stable (the difference in heats of formation is 9.4 kJ mol<sup>-1</sup>). The stability of the conformers increases

by 12 kJ mol<sup>-1</sup> as the location of the hydroxy group enhances the possibility of intramolecular hydrogen bond formation. It is worth mentioning that, according to the PM3 level of theory, molecules with a carbonyl group in the benzylidene moiety are not preferred. It seems that the formation of the intermolecular hydrogen bonding with the adjacent molecule results in an effective low-energy structure. This structure, with two perpendicular molecules, was calculated and we found that heat of formation was stabilized by 31 kJ mol<sup>-1</sup> compared with the two independent molecules.

## REFERENCES

1. March J. *Advanced Organic Chemistry*. Wiley: New York, 1992.
2. Cohen MD, Flavin SJ. *J. Chem. Soc. B*. 1967; 334.
3. Aldoshin CM, Atowmian LO. *Chim. Phys.* 1984; **3**: 915.
4. Connor JA, Kennedy RJ, Daves HM, Hursthouse MB, Walker NPC. *J. Chem. Soc. Perkin. Trans.* 1990; **2**: 203–207.
5. Lycka A. *Annu. Rep. NMR Spectrosc.* 1993; **28**: 248–281.
6. Wozniak K, He H, Klinowski J, Jones W, Dziembowska T, Grech E. *J. Chem. Soc., Faraday Trans.* 1995; **91**: 77–85.
7. Sitkowski J, Dziembowska T, Grech E, Stefaniak L, Webb GA. *Pol. J. Chem.* 1994; **68**: 2633–2636.
8. Zheglova DK, Gindin V, Koltsov AJ. *J. Chem. Res. (S)* 1995; 32–33.
9. Salman SR, Lindon JC, Farraut RD, Carpenter TA. *Magn. Reson. Chem.* 1993; **31**: 991–994.
10. Harris RK, Jonsen P, Packer KJ, Campbell CD. *Magn. Reson. Chem.* 1986; **24**: 977–983.
11. Elerman Y, Elmali A, Atakol O, Svoboda I. *Acta. Crystallogr. Sect. C* 1995; **51**: 2344–2346.
12. Kristek F, Klicnar J, Vetesnik P. *Collect. Czech. Chem. Commun.* 1971; **38**: 3608.
13. Walker J, Stuart J. *Acta. Crystallogr. Sect. A* 1983; **39**: 158.
14. Sheldrick GM. *SHELXL93. Program for the Refinement of Crystal Structure*. University of Göttingen: Göttingen, 1993.
15. Sheldrick GM. *Acta. Crystallogr. Sect. A* 1990; **46**: 467.
16. *International Tables for X-Ray Crystallography*, vol. IV. Kynoch Press: Birmingham, 1974.
17. Dziembowska T, Szczodrowska B, Krygowska TM, Grabowski S. *J. Phys. Org. Chem.* 1994; **7**: 142–146.
18. Krygowski TM. *J. Chem. Inf. Comput. Sci.* 1993; **33**: 70–78.